SINTEF
PROCEEDINGS
2

Proceedings of the 12th International Conference on Computational Fluid Dynamics in the Oil & Gas, Metallurgical and Process Industries

Progress in Applied CFD – CFD2017

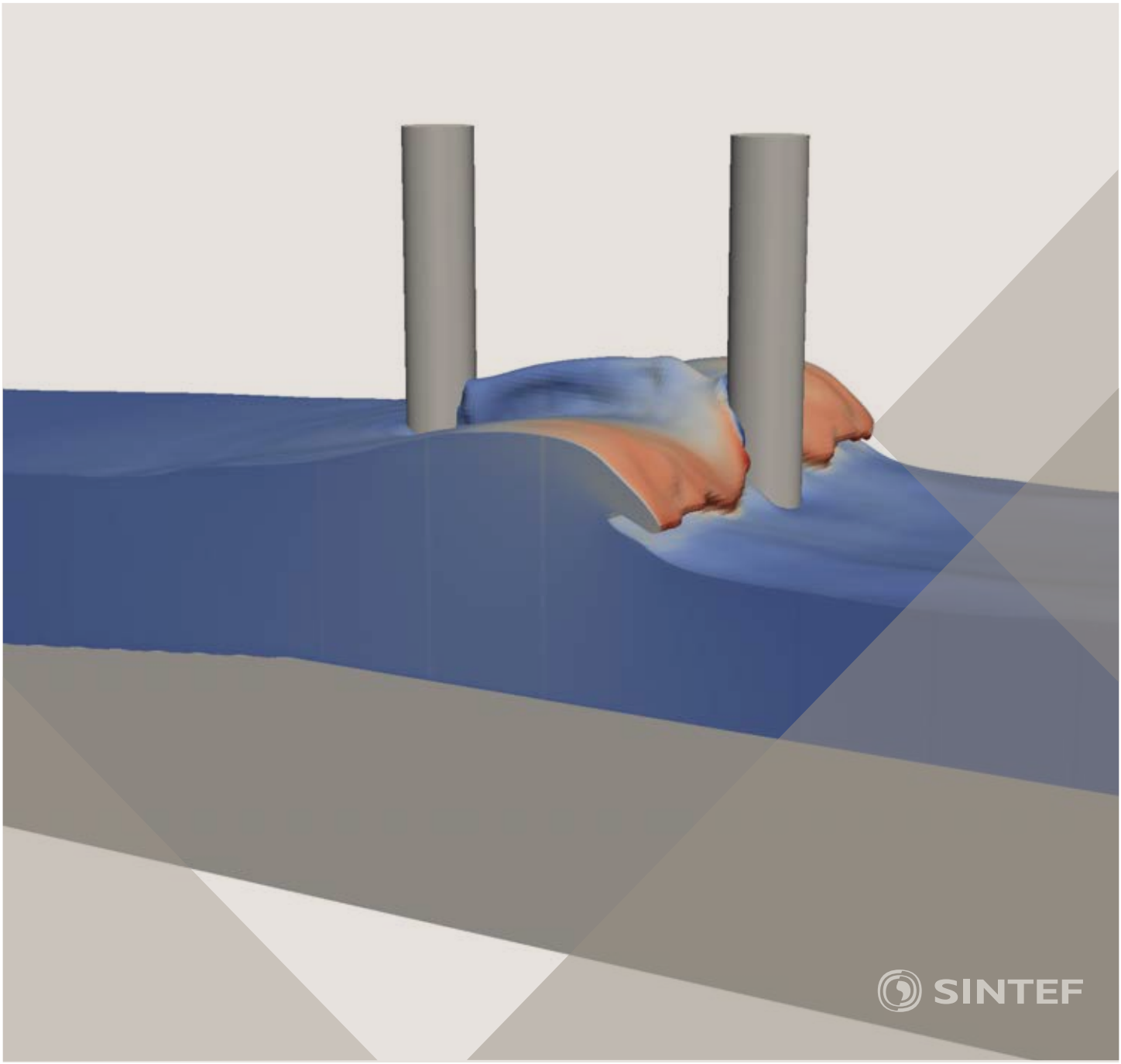

SINTEF Proceedings

Editors:
Jan Erik Olsen and Stein Tore Johansen

Progress in Applied CFD – CFD2017

Proceedings of the 12th International Conference on Computational Fluid Dynamics in the Oil & Gas, Metallurgical and Process Industries

SINTEF Academic Press

SINTEF Proceedings no 2
Editors: Jan Erik Olsen and Stein Tore Johansen
Progress in Applied CFD – CFD2017
Selected papers from 10th International Conference on Computational Fluid Dynamics in the Oil & Gas, Metallurgical and Process Industries

Key words:
CFD, Flow, Modelling

Cover, illustration: Arun Kamath

ISSN 2387-4295 (online)
ISBN 978-82-536-1544-8 (pdf)

SINTEF Academic Press
Address: Forskningsveien 3 B
PO Box 124 Blindern
N-0314 OSLO
Tel: +47 73 59 30 00
Fax: +47 22 96 55 08

www.sintef.no/byggforsk
www.sintefbok.no

SINTEF Proceedings
SINTEF Proceedings is a serial publication for peer-reviewed conference proceedings on a variety of scientific topics.
The processes of peer-reviewing of papers published in SINTEF Proceedings are administered by the conference organizers and proceedings editors. Detailed procedures will vary according to custom and practice in each scientific community.

PREFACE

This book contains all manuscripts approved by the reviewers and the organizing committee of the 12th International Conference on Computational Fluid Dynamics in the Oil & Gas, Metallurgical and Process Industries. The conference was hosted by SINTEF in Trondheim in May/June 2017 and is also known as CFD2017 for short. The conference series was initiated by CSIRO and Phil Schwarz in 1997. So far the conference has been alternating between CSIRO in Melbourne and SINTEF in Trondheim. The conferences focuses on the application of CFD in the oil and gas industries, metal production, mineral processing, power generation, chemicals and other process industries. In addition pragmatic modelling concepts and bio-mechanical applications have become an important part of the conference. The papers in this book demonstrate the current progress in applied CFD.

The conference papers undergo a review process involving two experts. Only papers accepted by the reviewers are included in the proceedings. 108 contributions were presented at the conference together with six keynote presentations. A majority of these contributions are presented by their manuscript in this collection (a few were granted to present without an accompanying manuscript).

The organizing committee would like to thank everyone who has helped with review of manuscripts, all those who helped to promote the conference and all authors who have submitted scientific contributions. We are also grateful for the support from the conference sponsors: ANSYS, SFI Metal Production and NanoSim.

Stein Tore Johansen & Jan Erik Olsen

Organizing committee:

Conference chairman: Prof. Stein Tore Johansen
Conference coordinator: Dr. Jan Erik Olsen
Dr. Bernhard Müller
Dr.Sigrid Karstad Dahl
Dr.Shahriar Amini
Dr.Ernst Meese
Dr.Josip Zoric
Dr.Jannike Solsvik
Dr.Peter Witt

Scientific committee:

Stein Tore Johansen, SINTEF/NTNU
Bernhard Müller, NTNU
Phil Schwarz, CSIRO
Akio Tomiyama, Kobe University
Hans Kuipers, Eindhoven University of Technology
Jinghai Li, Chinese Academy of Science
Markus Braun, Ansys
Simon Lo, CD-adapco
Patrick Segers, Universiteit Gent
Jiyuan Tu, RMIT
Jos Derksen, University of Aberdeen
Dmitry Eskin, Schlumberger-Doll Research
Pär Jönsson, KTH
Stefan Pirker, Johannes Kepler University
Josip Zoric, SINTEF

CONTENTS

EXPERIMENTAL AND CFD INVESTIGATIONS OF FRACTAL DISTRIBUTOR ON A NOVEL PLATE AND FRAME ION-EXCHANGER

Gonggiang He[1],Vadim Kochergin[2], Yuehao Li[1], Krishnaswamy Nandakumar[1]*

[1] Louisiana State University, Baton Rouge, LA, USA
[2] Amalgamated Research LLC (ARi), ID, USA

* E-mail: nandakumar@lsu.edu

ABSTRACT

Conventional pressure based flow distributors face challenges in the form of operational limits as their low outlet density and non-uniform flow distribution path, often act as bottleneck in the overall chemical equipment efficiency. Recently, a new distributor design inspired by the concept of fractal shows promising performance over a wide range of applications and operating conditions. The inherent scaling symmetry from such fractal distributors allows identical hydraulic flow path length to all outlets as well as much higher outlet density. In this study, we have designed a novel 12" by 12" plate and frame type ion-exchanger called "Fractal Pack" and tested it in pilot scale adopting fractal distributors with 256 outlets under operating flow rates ranging from 6.31×10^{-5} m3/s to 2.52×10^{-4}m3/s. For comparison, ion-exchanger with 16 distributor outlets has also been assembled to mimic the performance of conventional pressure-based design. Both residence time distribution test and CFD investigations have been conducted. From CFD results, at highest flow rate, we found the overall pressure drop for ion-exchanger with 16 outlets is about 6 times larger than with fractal distributor and 78% of its pressure drop is caused by sudden expansion and contraction at 16 outlets. In addition, a key index, degree of heterogeneity which measures the percentage of mal-distribution zones inside resin, has been defined to quantify flow distribution inside resin. The distributor equipped with 16 outlets shows 4 times more mal-distribution zones than 256 outlets at highest flow rate. This work demonstrates that fractal distributors can reliably provide superior performance over conventional distributors in a compact design framework; by introduction of symmetry, fractal distributors can aid process intensifications for many chemical processes that are plagued by heterogeneities and poor process efficiencies. The work also demonstrates how CFD can assist in avoiding ad-hoc design decision on dimensions and systematically explore the design space for optimum design decisions, using optimization criteria like coefficient of variation, degree of dispersion or heterogeneity.

Keywords: CFD, flow distribution, fractal geometry, fluid distributor, RTD

NOMENCLATURE

Greek Symbols

α Permeability, [m^2].
δ_{ij} Kronecker delta function.
ϵ Turbulence energy dissipation rate, [m^2/s^2].
μ Dynamic viscosity, [kg/m.s].
μ_t Turbulent viscosity, [kg/m.s].
ρ Mass density, [kg/m^3].
σ Turbulent Prandtl number.

Latin Symbols

C Tracer concentration, [mol/m^3].
d Channel depth, [m].
D_d Diffusivity of the tracer, [m^2/s].
D_p Diameter of resin bead, [m].
g Gravity, [m/s^2].
G_k Generation of turbulent kinetic energy due to the mean velocity gradients, [m^2/s^2].
G_b Generation of turbulent kinetic energy due to buoyance, [m^2/s^2].
h Channel width, [m].
k Turbulent kinetic energy, [m2/s2].
p Pressure, [Pa].
R Resistance in the resin section, [Pa/m].
u_i Velocity component in i^{th} spatial component, [m/s].
x_i i^{th} spatial component, [m].

Sub/superscripts

i Index *i.*
j Index *j*.
$\rightarrow$ Vector form.

INTRODUCTION

Since its emergence in 1970s, process intensification, as one promising innovation paths in chemical process industry, has been attracting extensive research interests from both academic and industrial sectors. Process intensification consists of the development of novel apparatuses and techniques that can lead to drastic improvement in chemical processes by reduction of equipment size, energy consumption or water utilization. Such characteristics are highly desired as they make the chemical industry more sustainable and environment-friendly(H. Liu et al., 2010). One good topic of process intensification is the innovation of flow distributors(V. Kochergin and M. Kearney, 2006). Flow distributors are extensively integrated by chemical equipment to distribute incoming feed streams uniformly

prior to the subsequent operations, whether it is reaction, mixing or separation. The efficiency of the flow distributor plays a key role in determining the overall performance of the chemical equipment. When the distributors have low efficiencies, the chemical equipment has to be oversized as a compensation, resulting in increased material and energy consumption and reduced efficiency. In order to achieve process intensification, innovative flow distributors that offer uniform flow distribution and close residence time distribution of the feed streams are in urgent need by the chemical industry.

Conventional flow distributors utilize the pressure-based and trough-type designs, of which the typical diagrams are shown in Figure 1(a) and (b), respectively. The pressure-based designs, i.e., spray nozzle distributors as seen in Figure 1(a), positions their outlets on the branches with certain interval. The flow paths from the distributor to each outlet are varying between each other. In order to achieve uniform flow distribution, each outlet has to be sized accordingly based on its flow paths. Such design concept is associated with several inherent disadvantages. As the outlet are designed based on particular operating flow rates, the performance of such distributors are undermined when the operating flow rates deviate from the designed value significantly. For example, the process fluid may drip only from those center outlets when the operating flow rate is much lower than the designed one. In addition, the varying flow path results in different residence time of each stream. Furthermore, the scale-up of such distributors requires significant efforts as the design lacks symmetry. The outlet density, which is defined as the number of outlets per unit cross-sectional area, is usually limited below 250 openings per square meters(V.J. Inglezakis and S.G. Poulopoulos, 2006).

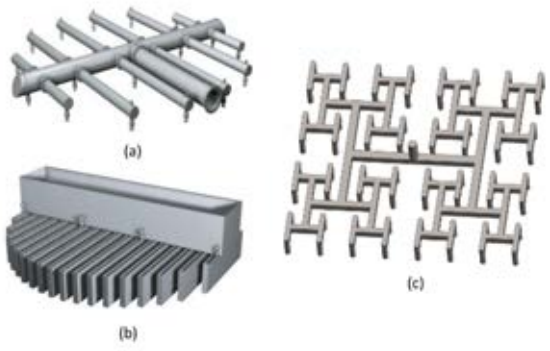

Figure 1 (a) a conventional spray nozzle distributor (Sulzer Chemtech Ltd). (b) A trough-type liquid distributor (Sulzer Chemtech Ltd). (c) A fractal distributor

First proposed in 1994 (M.M. Kearney et al., 1994), fractal distributors are now attracting extensive research interests. Such distributors are inspired by the fractal patterns existing in nature, i.e., human's lung systems, leaf veins and river basins. The key feature shared by fractal patterns is the self-similarity (B. Mandelbrot, 1982). In other words, these patterns contain pieces that are duplications of the same pattern on successively increasing finer scales. By adopting such a feature in engineering, fractal distributors utilize symmetric pipe systems to distribute fluid flow as seen in Figure 1(c). Since such designs rely on the symmetry rather than pressure drop or hydraulic head, they show superior performances over conventional distributors in various aspects. First, the fractal distributor allows easy scale up due to the self-similarity feature; as a result, the distributors can achieve much higher outlet density than conventional distributors. Second, the feed streams have close residence time distribution, as their flow paths are almost identical. In addition, fractal patterns regulate turbulent eddies by subdividing large eddies into smaller ones. The flow lamination helps to improve the homogeneity in the downstream chemical equipment.

In this study, we present our experimental and CFD investigations of a novel fractal distributor integrated into a "fractal pack" based ion exchanger. Such an ion exchanger consists of multiple plates fabricated by poly-methyl- methacrylate (PMMA). The internal channels of the fractal are machined inside PMMA plates. The distributor was assembled with either 16 or 256 outlets. The 16-outlet distributor mimics the outlet density of a conventional pressure-based design. However, it is noted that the 16-outlet design used in this study is still a fractal configuration and includes the benefits of hydraulic symmetry to all outlets. Therefore, for this paper, the 16-outlet distributor can be considered a "best case" pressure-based design. Conventional pressure-based designs, such as spray nozzle distributors, would be expected to perform in a less favourable manner than presented here for the 16 outlet fractal device. There are three aims of this work: (1) to develop and validate a CFD model that captures the fluid flow inside the fractal distributor and other components of the ion exchanger; (2) to compare the performance of a fractal distributor with a "best case" hydraulically symmetric pressure-based distributor; (3) to explore design space for optimizing fractal distributor performance, using optimization criteria like coefficient of variation in flow rate.

EXPERIMENTAL SETUP

In collaboration with Amalgamated Research LLC, a novel ion exchanger at pilot scale was fabricated using PMMA. As shown in Figure 2, such exchanger is composed by three components: a fractal distributor, a resin exchanging bed and a fractal collector. The detailed illustrations of each component are shown in Figure 2. The fractal distributor is assembled by three plates. The 1st plate consists of an H-shape channel which distributes the incoming fluid stream from the fractal inlet to 4 outlets. Leaving those outlets, the distributed fluid streams then enter the 2nd plate where they are distributed again to 16 outlets. Similarly, the incoming fluid streams are again further distributed to 256 outlets on the 3rd plate. Each outlet in the 3rd plate has a cone-shape expansion which maximizes the contact area between the distributed stream and the resin bed downstream. These plates were assembled carefully to ensure that the outlets of the previous plate were aligned to the inlets of the next plate precisely.

After the fluid streams leave the fractal distributor, they enter the resin red as shown as plate 4 in Figure 2. The resin bed is comprised by 310-micron ion-exchange resin beads which are confined inside the resin frame. The porosity of the resin bed is about 0.44. The particular

ion exchange resin used in these tests does not adsorb food dye (FD&C Blue No.1) and only acts as a simple porous media for RTD and visualization testing. Post to the resin section, the fluid streams are collected by a fractal collector. Such a collector is identical to the fractal distributor, but the three plates (5th, 6th, and 7th) are assembled in a reverse order. The process streams merge from these inlets into one. The thickness of each plate in the distributor and the collector is about 25.3 mm.

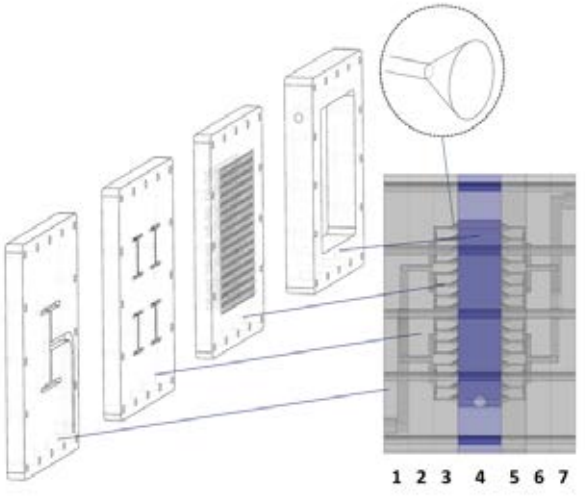

Figure 2 Schematic view of the ion-exchange system: (1) the 1st plate consisting of one inlet and H-shape channel with four outlets; (2) the 2nd plate consisting of 16 outlets; (3) the 3rd plate consisting of 256 outlets with cone shape expansion; (4) resin frame where resin is stuffed inside; (5), (6) & (7) collector plates with identical structure as those in the distributor but in a reverse direction.

The flow visualization experiment and the residence time distribution (RTD) analyses were carried out during the experiments to visualize the fluid flow inside the fractal distributor.

MODEL DESCRIPTION

As the process fluid satisfies the incompressible and Newtonian conditions, the fluid flow can be described by the incompressible Navier-Stokes equations. The Reynolds number in the fractal inlet, corresponding to flow rate as 2.52 x10^{-4} m^3/s, is 14400 ($Re = \rho U D_h/\mu$, in which ρ is fluid density; U is the superficial velocity in the inlet; Dh is the hydraulic diameter of the inlet; μ is fluid viscosity), indicating that the flow is in the fully-developed turbulent regime. Therefore, the Reynolds-averaged Navier-Stokes (RANS) equations were adopted to describe the turbulent flow:

$$\frac{\partial}{\partial x_i}u_i = 0 \tag{1}$$

$$\rho\frac{\partial}{\partial x_j}(u_i u_j) = -\frac{\partial}{\partial x_i}p + \frac{\partial}{\partial x_j}\left[\mu\left(\frac{\partial}{\partial x_j}u_i + \frac{\partial}{\partial x_i}u_j\right)\right] - \rho\frac{\partial}{\partial x_j}\left(\overline{u_i' u_j'}\right) + \rho\vec{g} + \vec{R} \tag{2}$$

in which u is the mean velocity vector, and the subscripts i, j and k stand for the components on x, y and z directions; x is the spatial vector; ρ is fluid density; p is pressure; μ is fluid viscosity; u_i' and u_j' are the fluctuating velocity components; $\vec{g}$ is the gravitational vector; and $\vec{R}$ is the resistance in the resin section which is estimated by the Ergun equation.

In order to close the RANS equations, the Reynolds stresses term, $-\rho\left(\overline{u_i' u_j'}\right)$, are modeled by employing the Boussinesq hypothesis:

$$-\rho\overline{u_i' u_j'} = \mu_t\left(\frac{\partial}{\partial x_j}u_i + \frac{\partial}{\partial x_i}u_j\right) - \frac{2}{3}\left(\rho k + \mu_t\frac{\partial}{\partial x_k}u_k\right)\delta_{ij} \tag{3}$$

in which μ_t is the turbulent viscosity; k is the turbulent kinetic energy; δ_{ij} is the unit component in the stress tensor.

In this study, μ_t and k are estimated by the realizable k-ε model. Compared to the standard k-ε model, the realizable k-ε model modifies the ε equation to improve the accuracy of predicting turbulent kinetic energy dissipation rate. Therefore, it shows superior abilities to capture complex flow structures in fractal channels. The model remains valid at low Reynolds number flow regions where k, ε and hence μ_t tend to zero with fluid flow determined solely by NSE model.

The realizable k-ε model solves two transport equations for the turbulence kinetic energy k and its dissipation rate ε:

$$\rho\frac{\partial}{\partial x_j}ku_j = \frac{\partial}{\partial x_j}\left[\left(\mu + \frac{\mu_t}{\sigma_k}\right)\frac{\partial}{\partial x_j}k\right] + G_k + G_b - \rho\varepsilon \tag{4}$$

$$\rho\frac{\partial}{\partial x_j}\varepsilon u_j = \frac{\partial}{\partial x_j}\left[\left(\mu + \frac{\mu_t}{\sigma_\varepsilon}\right)\frac{\partial}{\partial x_j}\varepsilon\right] + \rho C_1 S\varepsilon - \rho C_2\frac{\varepsilon^2}{k+\sqrt{\nu\varepsilon}} + C_{1\varepsilon}\frac{\varepsilon}{k}C_{3\varepsilon}G_b \tag{5}$$

and the turbulent viscosity μ_t is computed by

$$\mu_t = \rho C_\mu k^2/\varepsilon \tag{6}$$

In the above equations, G_k and G_b are the generation of turbulent kinetic energy due to the mean velocity gradients and buoyance, respectively; $\sigma_k = 1.0$ and $\sigma_\varepsilon = 1.2$ are the turbulent Prandtl number for k and ε, respectively; $C_{1\varepsilon} = 1.44$ and $C_2 = 1.9$ are the model constants. The detailed expression of G_k, G_b, C_1, S and other variables can be found in the reference(T.-H. Shih et al., 1995).

In the resin section, the porous media exerts strong resistance to the fluid flow. Such resistance is accounted into the RANS equations as a source term, $\vec{R}$. The component of $\vec{R}$ is estimated by the classic Ergun equation as:

$$R_i = -\left(\frac{\mu}{\alpha}u_i + C_{R2}\rho|u_i|u_i\right) \tag{7}$$

in which α is the permeability, and C_{R2} is the inertial resistant coefficient. They are expressed as:

$$\alpha = \frac{D_p^2}{150}\frac{\epsilon^3}{(1-\epsilon)^2} \tag{8}$$

$$C_{R2} = \frac{3.5}{D_p}\frac{(1-\epsilon)}{\epsilon^3} \tag{9}$$

Where, D_p is the diameter of resin bead, which is 310 μm; ϵ is the porosity of the resin section, which is 0.44.

The RTD analyses in the model were conducted by solving the species transport equation:

$$\frac{\partial}{\partial t}C + \frac{\partial}{\partial x_i}(u_i C) = D_d\frac{\partial}{\partial x_i}\left(\frac{\partial}{\partial x_i}C\right) \tag{10}$$

in which C is concentration of tracer; u_i is the velocity vector predicted by the N-S equations, and D_d is the diffusivity of the tracer which is specified as 4x10^{-5} m^2/s.

CFD SIMULATION SETUP

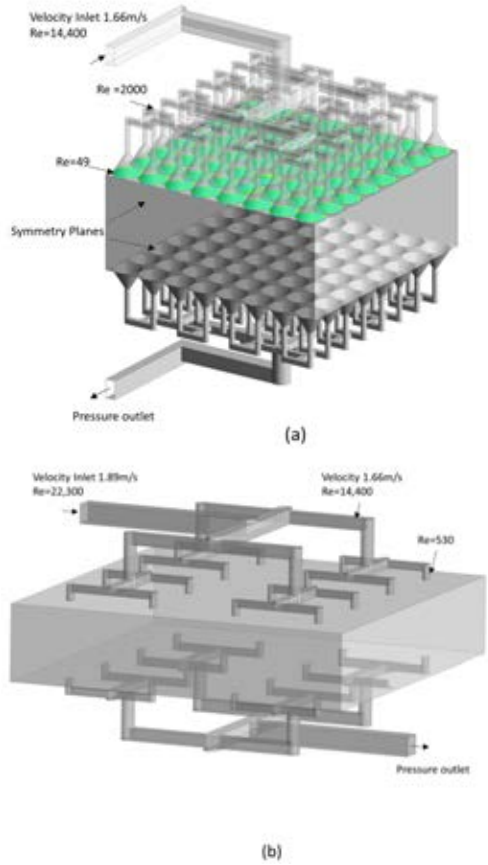

Figure 3 Illustration about the computational domains of the two ion exchangers: (a) The 1st ion exchanger with the fractal distributor of 256 outlets in total and only ¼ part (64 outlets) has been shown as computation domain. (b) The 2nd ion exchanger with the fractal distributor of 16 outlets. The typical Re in certain locations of the distributors are denoted in the figures.

The computational domain of the two ion exchangers is shown in Figure 3. The corresponding fractal distributors used by these two exchangers consist of 256 and 16 outlets, respectively. For the one of 256 outlets, only a quarter of the ion exchanger was simulated utilizing the symmetry condition. The location of symmetry planes have been shown in Figure 3(a). The inlet velocity was 1.660 m/s, corresponding to the volumetric flow rate of 2.52 $x10^{-4}$ m^3/s. For one of 16 outlets, the entire ion exchanger was simulated. The inlet velocity was specified as 1.89 m/s with same flow rate. The geometry of distributor with 16 outlets was created in a way that it followed the same dimension with the main branches from the distributor with 256 outlets, but without further splitting of outlets from 16 to 256 at the last horizontal plane.

The outlets of the collectors were specified as the pressure outlet with 0 Pa. No-slip conditions incorporating with the scalable wall function were specified to all wall boundaries. Dimensionless wall distance(y plus) vary around 20-10 based on local flow field and Re.

The SIMPLE (Semi-Implicit Method for Pressure-Linked Equations) scheme was used to couple the momentum and continuity equations. For spatial discretization, least-squares cell-based method was adopted for gradient; standard method, which interpolates the pressure on the faces using the cell center values, was used for pressure interpolation; second-order upwind was used for momentum, turbulent kinetic energy and turbulent dissipation rate.

All simulations have been performed with ANSYS FLUENT 16 with 40 processors on Supermike HPC located at Louisiana State University. The steady-state solutions of the N-S equations were obtained usually within 5000 iterations with convergence criteria at 1E-4. Then the corresponding velocity field from steady state solution was supplied to the species transport equation, which adopted transient simulations. A typical time step used by the simulations was 0.005s. The entire simulation took about 10 hours.

MODEL VALIDATION

The CFD model is validated by comparing the predicted RTD curves and pressure drops of the ion exchanger with the ones from the experiments. The simulations and the experiments were carried out with the two ion exchangers shown in Figure 4. Figure 4(a) plots the RTD curves predicted by simulations and the corresponding ones measured from experiments. The good agreement between the model and experiments suggests that the model successfully captured the flow inside the ion exchangers.

In this study, a mesh dependence test was performed prior to the parametric study in order to eliminate the potential numerical error resulted from the insufficient grid resolutions. Three types of grids with different resolutions were generated by the CutCell algorithm in Ansys Meshing. Figure 4(b) shows Velocity profiles along the sampling lines in the 1 ion exchanger with three mesh densities. The test results suggested that the flow profile in resin became independent from grid solutions when the total mesh elements exceeded 2.7 million. Therefore, such a mesh was selected for the following parametric studies.

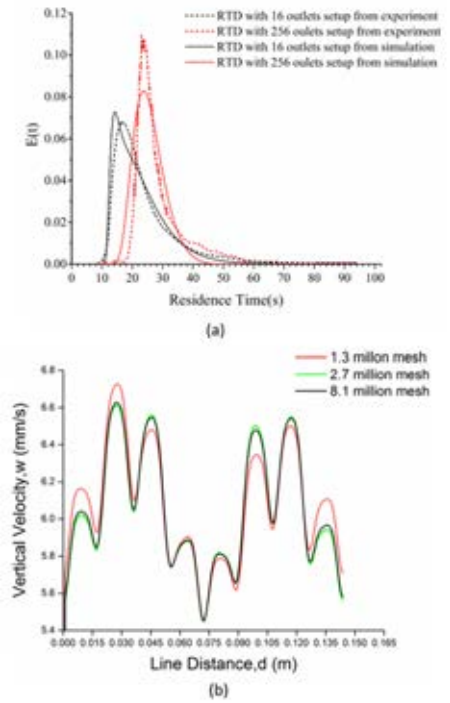

Figure 4 (a) Comparison of the RTD curves of the 1st and 2nd ion exchangers measured from experiments and predicted by the CFD simulations. The mesh with 2.7 million elements has been adopted for 1st ion exchanger. The exchangers were operated with a flow rate of 6.31E-5 m3/s. (b) Vertical velocity profiles along the sampling lines (cross line at 5mm depth inside resin) in the 1st ion exchanger with three mesh densities.

VELOCITY PROFILE COMPARISON OF TWO DISTRIBUTORS

In this section, we will compare the performance of a fractal distributor with a "best case" hydraulically symmetric pressure-based distributor.

In order to understand how the flow distribution influences the performance of ion exchangers, the detail flow profiles inside the resin bed were analysed with the aid of simulation results. For both 1st and 2nd distributor, the simulations were performed with same flow rate (2.52×10^{-4} m^3/s).Taking the 1st ion exchanger as an example, Figure 5 shows the overview of velocity profiles on three representative planes of the resin bed. The locations of these three planes are denoted in Figure 5(a). They are Plane 1 which is the top surface of the resin bed (0 mm), Plane 2 which is 5 mm below the top surface and Plane 3 which is 15 mm below.

In order to observe the velocity evolution quantitatively, three lines were sampled along the diagonal of planes of different depths as illustrated in Figure 6(a). The locations of these lines are denoted in Figure 5(a). They locate on the planes that are 5, 10 and 15 mm below the top surface of the resin bed, respectively. The corresponding velocity profiles plot in Figure 5(b) clearly demonstrates the homogenizing process of the velocity profiles along the transversal flow direction. When the process streams enter the resin bed, the fluid elements tend to take the shortcut to travel through the resin bed. Those regions on the flow track have large velocity magnitudes while the other regions off the track have lower ones. As a result, the velocity profiles shows fluctuations in magnitude, of which the maximum variation is about 1.20 mm/s. On the other hand, the resistant force exerted by the resin bed tends to homogenize the velocity profile. As indicated in Figure 6(b), the peak values is reduced along the transversal direction due to the resistance force. When the process stream reaches 15 mm plane, the maximum velocity variation is reduced to 0.25 mm, indicating that the flow profile approaches the plug pattern.

Figure 6 (c) compares the velocity profiles of the 1st and 2nd ion exchanger sampled at 5 mm plane with ¼ part of the whole domain. Clearly, the velocity profile of the 2nd ion exchanger shows a much larger variation than that of the 1st ion exchanger. The significant velocity variation is due to the inefficient initial distribution. As a result, the 2nd ion exchanger requires a much deeper resin bed than that of the 1st ion exchanger so as to attain a uniform velocity profile. On the other hand, the large velocity variation results in malfunctioning operations in the resin bed.

MALFUNCTIONING OPERATIONS OF THE RESIN BED

As illustrated in Figure 6, the inefficient distribution of the process stream causes significant variations in velocity profiles. Consequently, it leads to the malfunctioning operations of the resin bed such as "dead space" and "channelling".

The term "dead space" is commonly used in industry to name those regions where the fluid elements have

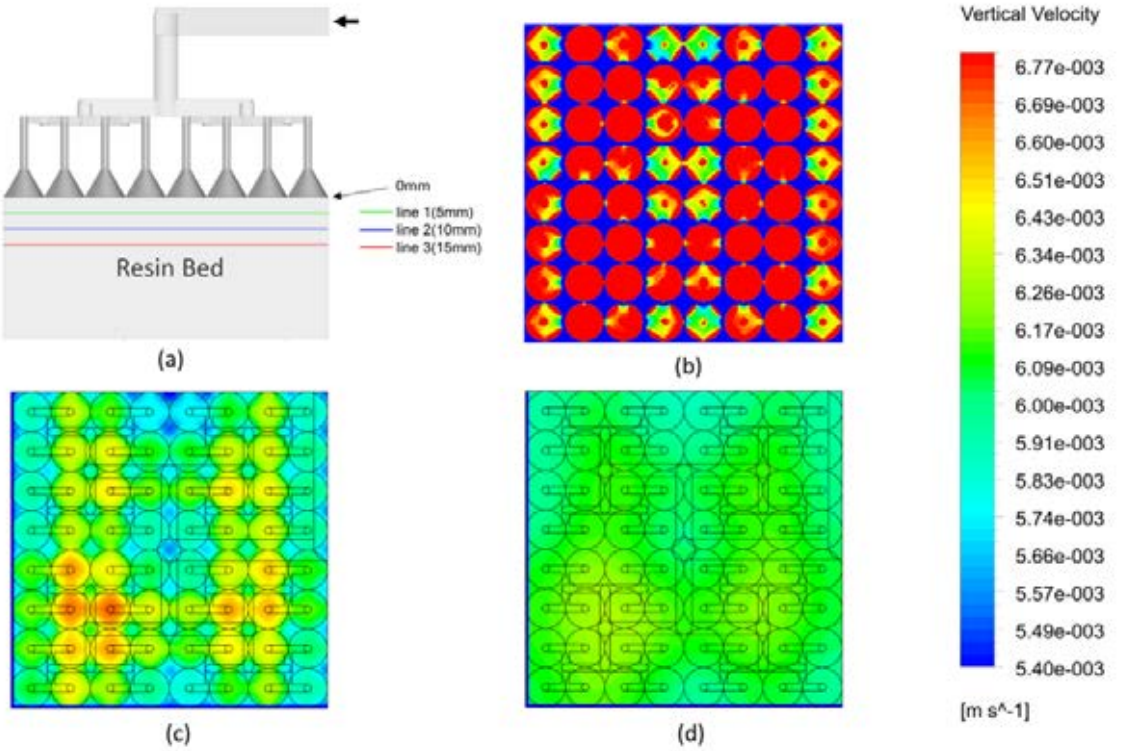

Figure 5 (a) Locations of the three representative planes: Plane 1 which is the top surface of the resin bed (0 mm), Plane 2 which 5 mm below the top surface and Plane 3 which is 15 mm below the top surface. (b), (c) and (d): Contours of vertical velocity in the flow direction on Plane 1, Plane 2 and Plane 3, respectively.

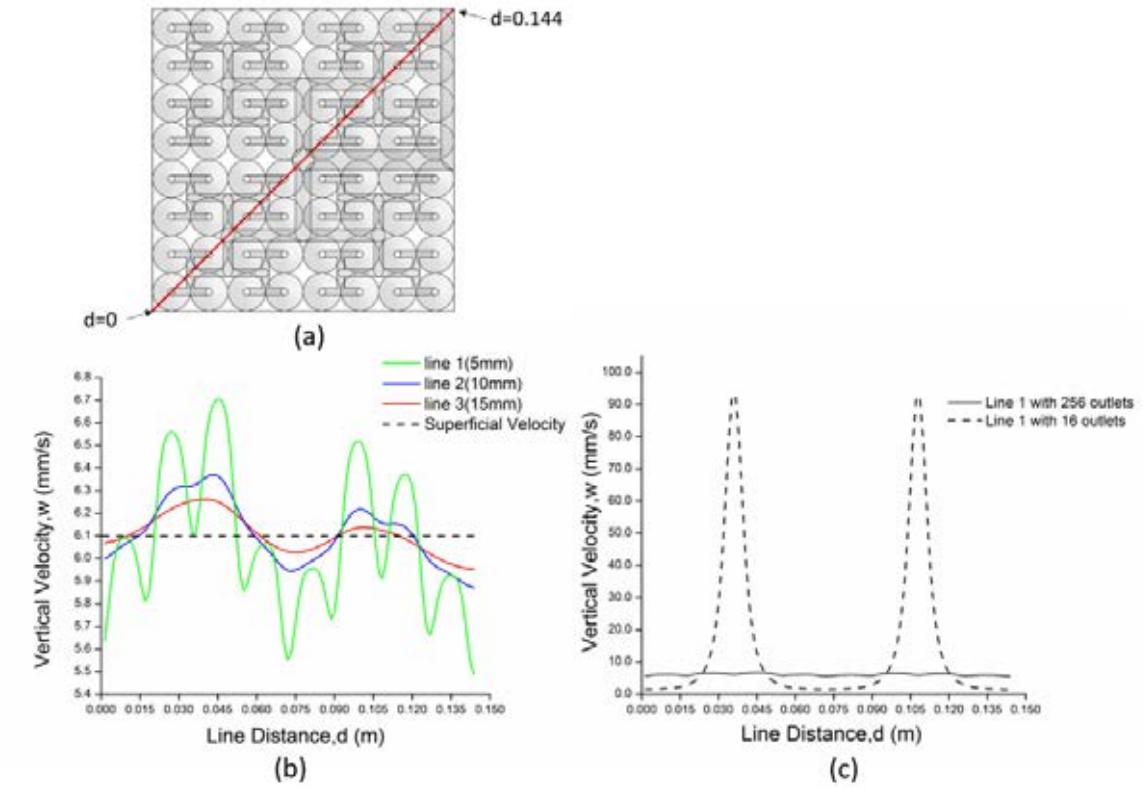

Figure 6 (a) Illustration about the location of the sampling lines. (b) Velocity profiles along the sampling lines in the 1st ion exchanger. (c) Comparison of velocity profiles along Line 3 between the 1st and 2nd ion exchangers.

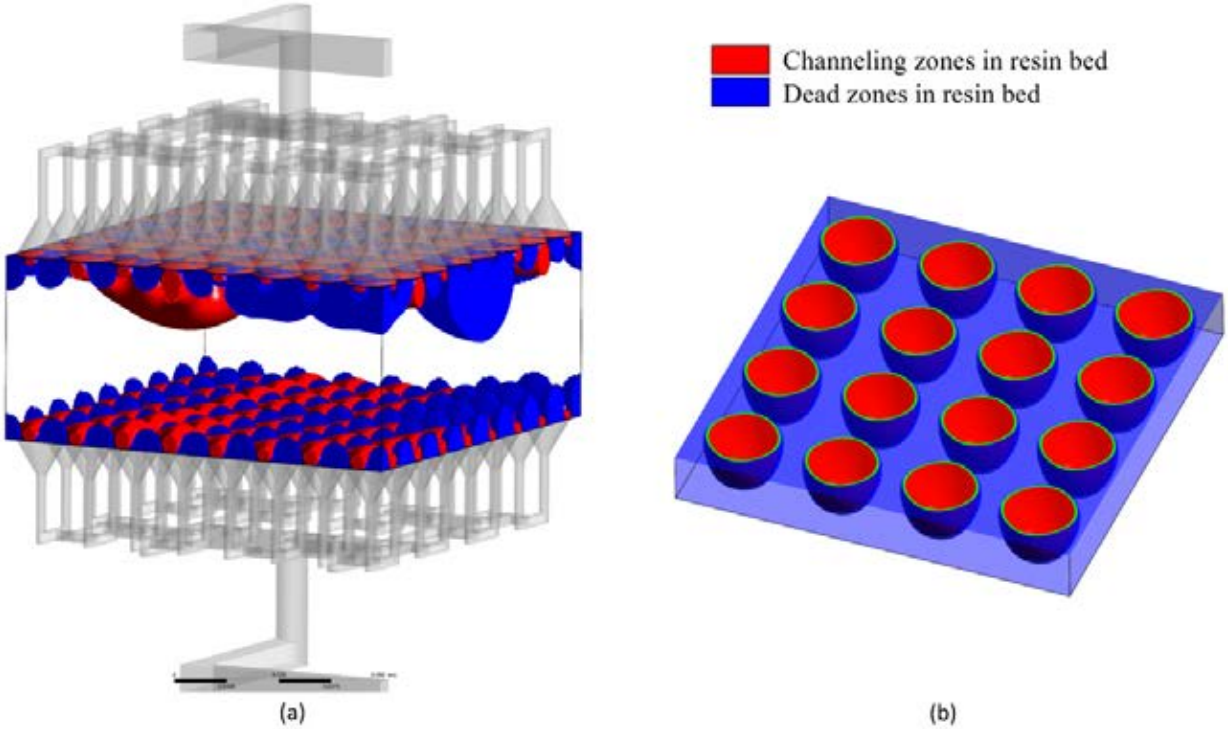

Figure 7 Locations of the malfunctioning zones in (a) the 1st and (b) the 2nd ion exchangers.

much lower velocities than the superficial velocity. In the dead space, the fluid elements have prolonged residence time due to their low velocities. Herein, the dead space is defined as the region where the velocity magnitude of the process stream is 2.5% below the superficial velocity. In contrast, "channelling" refers to the phenomenon that fluid passes through bed prematurely with a much shorter residence time. A zone with the fluid velocity that is 2.5% over the superficial one is defined as "channelling" zones. In order to quantify the malfunctioning operations, the volumetric percentages of the dead space and channelling zones were estimated based on the modelling results. For example, the percentage of the dead space is defined as:

$$\text{Dead space percent} = \frac{\text{volume of the dead space}}{\text{total volume of the resin bed}}$$

A universal index, "degree of heterogeneity", was used to evaluate the operation of the resin bed. The degree of heterogeneity is defined as the sum of dead space percentage and channelling zone percentage.

Figure 7 plots the corresponding locations of the dead space and channelling zones in the resin beds of the 1st and 2nd ion exchanger, respectively. The dead space is marked in blue while the channelling zone is in red. As discussed previously, the fractal distributor of the 1st ion exchanger provides efficient initial distribution. The velocity profile reaches plug flow within 15 mm of bed depth. Because of efficient initial distribution, the majority of the resin bed in the 1st ion exchanger shows normal operation as indicated in Figure 7(a). The malfunctioning zones appear only in the vicinity of the top and bottom surface of the resin bed where the flow has expansions and contractions due to the existence of the fractal distributor and collector. As shown in Table 1, the dead space takes 6.28% of the resin bed, and the channelling zones is 16.14%. The total degree of heterogeneity of the resin bed is 22.42%, indicating that the majority of the resin bed has uniform velocity distribution thus good operation.

In contrast, the resin bed in the 2nd ion exchanger has malfunctioning operations. As shown in Figure 7(b), the process streams leave the fractal distributor and travel through the resin bed with a high velocity. As a result, those regions in their flow track forms the channelling zone. According to Figure 7(b) and Table 1, the channelling zones spread from the fractal distributor to the fractal collector, taking up 22.97% of the resin bed. In contrast, a majority of the resin bed is dead space, taking up about 68.14% of the resin bed. The total degree of heterogeneity is 91.11%, suggesting that the entire bed is in malfunctioning.

Table 1 Summary of the malfunctioning zones

	Dead Space percentage	Channeling zone percentage	Degree of heterogeneity
1st Ion exchanger	6.28%	16.14%	22.42%
2nd Ion exchanger	68.14%	22.97%	91.11%

PRESSURE DROPS OF THE TWO ION EXCHANGERS

The pressure drop across the ion exchanger is an important parameter as it determines the required pressure head and subsequently operating cost. The modelling results indicate that the design of the fractal distributor impacts not only the velocity profiles in the resin bed but also the pressure drop across the ion exchanger. When the ion exchangers are operated with a flow rate of 2.52×10^{-4} m/s, the corresponding pressure drops across the fractal distributor and the resin bed are summarized in Table 2.

Table 2 Summary of the pressure drops across the ion exchangers

Pressure drop	Across the resin bed (Pa)	Across the entire ion exchanger (Pa)	Percentage of resin bed
1st Ion exchanger	8.1×10^3	1.6×10^4	51%
2nd Ion exchanger	9.9×10^3	9.7×10^4	10%

When these two ion exchangers were operated with same flow rate, the total pressure drop of the 1st one is only about 16% of the 2nd one. The pressure drops across the resin beds of these two ion exchangers are close to each other, and that of the 2nd ion exchanger is slightly higher due to the channelling zones and dead space. The modelling results suggest that the significant pressure drop in the 2nd ion exchanger is resulted from the sudden expansion and contraction of the process streams.

Figure 8 plots the pressure distributions inside the outlets of the fractal distributors in the 1st and 2nd ion exchangers. The fractal distributor equipped by the 1st ion-exchanger has a cone-shape expansion in its outlet. Such design provides a smooth expansion to the fluid; as a result, the corresponding pressure drop in the outlet is only about 270 Pa. In contrast, the outlets of the fractal distributor in the 2nd ion exchanger is designed with straight channels. Leaving the outlet, the process stream has a steep expansion. Such a steep expansion results in a significant pressure loss. The pressure drop of the outlet is about 3.7×10^4 Pa, which is almost two orders of magnitude higher than that of the 1st fractal distributor. The resin beads closed to outlets may be washed away in the real world. Although this phenomena cannot be captured in our lumped model, the steep expansion may still have significant impact on system pressure drop.

Based on the modelling results, one may conclude that the steep expansion of the streams leads to excessive pressure drop. As illustrated in Figure 1, the outlet designs in most of conventional distributors are similar to that of the 2nd fractal distributor. These conventional distributors inevitably result in large pressure drops. The modification of outlet design can reduce the pressure drop and subsequently saves the operating cost.

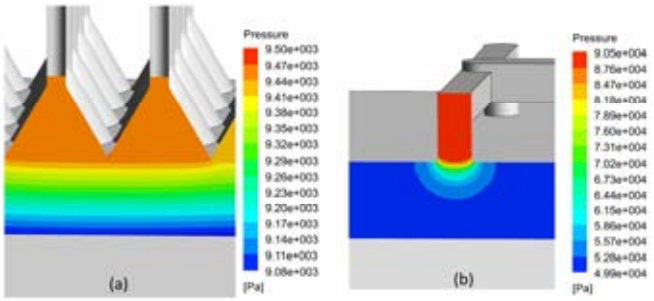

Figure 8 Pressure distributions in the outlets of (a) the fractal distributor of the 1st ion exchanger and (b) the fractal distributor of the 2nd ion exchanger.

COMPARISON OF THE RTDS OF THE TWO ION EXCHANGERS

According to the previous sections, the design of a fractal distributor determines the velocity profiles inside the resin bed. Due to the low outlet density of the 2nd fractal distributor, the velocity profile inside the resin bed of the 2nd ion exchanger is not uniform. A majority of the resin bed has dead space and channeling zones. In

order to understand the effect of outlet density on the residence time distribution (RTD) of process streams, RTD analyses were carried out with the two ion exchangers. The flow rate of the process stream was set as 6.31×10^{-5} m^3/s, and the resultant RTD curves are shown in Figure 9.

As discussed earlier, the fractal distributor in the 2nd ion exchanger cannot distribute the incoming process stream uniformly due to its low outlet density. The corresponding RTD curve confirms the existence of the channeling zone and the dead space. The mean residence time, tm, of the 2nd ion exchanger, which is 24.1 s, is smaller than that of the 1st ion exchanger. The smaller tm suggesting that a significant amount of tracer leaves the resin bed through the shortcut of channelling zones, which is generally known as "channelling" phenomenon. On the other hand, the curve has a long tail, suggesting that the corresponding the rest tracer elements have prolonged residence time due to the dead space. The dimensionless second moment, τ, which is defined as

$$\tau = \frac{\text{second moment } (\sigma^2)}{t_m^2}$$

evaluates the overall dispersion in RTD response. From the table in Figure 9, the 2nd ion exchanger has a larger τ than the 1st ion exchanger, indicating that the tracer is widely spread when it passes through the 2nd ion exchanger.

In comparison, the RTD curve corresponding to the 1st ion exchanger is close to that of a plug flow. The shape is close to symmetric response and has less dispersion. Such shape is consistent with the velocity profiles shown in Figures 5 and 6. As the velocity profiles become plug shape within a short distance, the tracer travels through the resin bed with fairly uniform residence time.

Based on Figure 9, one may conclude that the outlet density of a fractal distributor plays a key role in determining the performance of the downstream resin bed. Conventional pressure-based distributors are similar to the fractal distributor of the 2nd ion exchanger, which generally have low outlet densities. The low outlet density undermines the overall performance of the resin bed. In comparison, fractal distributors can achieve large outlet density easily because of the inherent scaling symmetry. Since they provide uniform distributions, the fractal distributors can ensure high efficiencies of resin beds with reduced dead space and narrower residence time distribution.

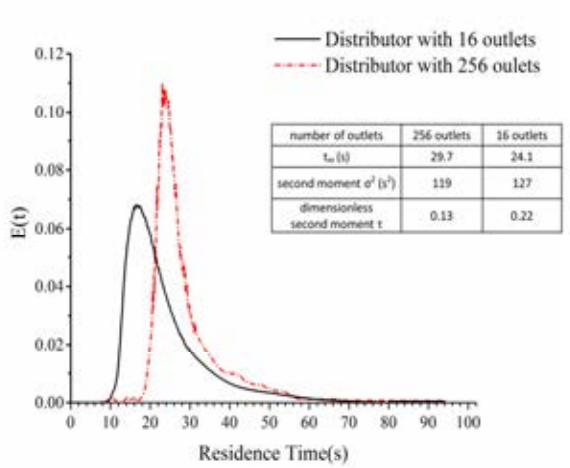

number of outlets	256 outlets	16 outlets
t_m (s)	29.7	24.1
second moment σ^2 (s^2)	119	127
dimensionless second moment τ	0.13	0.22

Figure 9 RTD curves of the 1st and 2nd ion exchangers operated with an incoming flow rate of 6.31×10-5 m3/s. The embedded table lists the mean residence time and second moments.

FRACTAL DISTRIBUTOR GEOMETRY FLOW UNIFORMITY OPTIMIZATION

CFD can assist in avoiding ad-hoc design decision on dimensions and systematically explore the design space for optimum design decisions.

In this section, the hydrodynamics of fractal distributor has been discussed. For simplification purpose, CFD fluid domain contains only main branches of previous fractal distributor geometry where the degree of preferential flow is higher. The modelling setup is very similar to the previous setup but zero pressure outlet boundary condition. Figure 10(a) show case the velocity vector distribution inside the original configuration at 3 GPM.

Parametric study has been performed with different scaling of width and depth based on previous configuration. For example, 0.625*d means all channel depth is 0.625 of previous design. With a total of 25 different configurations automatic generated from ANSYS WORKBENCH, we collected the coefficient of variation of flow rate at all outlets for each case. The response surface was plotted in Figure 10(b). From the result, we can conclude that 1) with channel depth fixed, decreasing channel width may improve flow uniformity. 2) with channel width fixed, increasing channel depth generally can increase the performance but there may be some optimized depth to width ratio.3) Since there is no back pressure at outlet, the Coefficient of Variation(CV) may overestimated in this setup. With addition of resin bed, CV values may drop significantly. However, the relative relationship of width and depth ratio to CV may still hold and the response surface offers a useful guide line for design of fractal distributor. 4) 1.265 as channel depth to width ratio (aspect ratio) is recommended for high flow distribution performance.

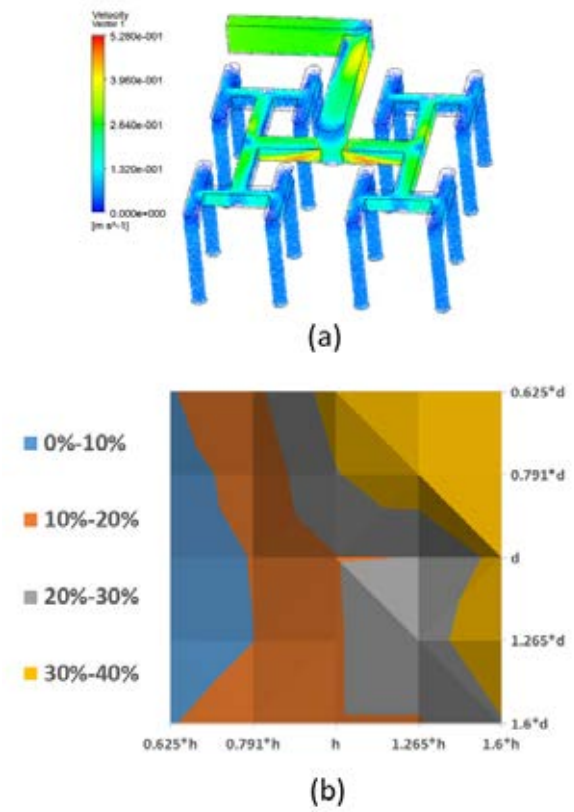

Figure 10 (a) velocity vector plot for flow rate at 3 GPM. (b) Response surface of coefficient of variation based on the flow rate at each outlet at 3GPM.

Conclusion

In this work, a novel filter press-based ion exchanger equipped with a fractal distributor and a fractal collector was fabricated using PMMA. Two ion exchanger configurations, of which the 1st one includes a fractal distributor of 256 outlets and the 2nd one with a fractal distributor of 16 outlets, respectively, were investigated by CFD simulations and experiments including residence time distribution (RTD) analysis and dye visualization experiments.

The results indicate that the outlet density of a fractal distributor plays a key role in determining the overall performance of an ion exchanger. When the fractal distributor has a high outlet density, the process stream reaches a uniform velocity profile similar to a plug flow with a short depth inside the resin bed. As a result, the process stream has a uniform residence time distribution in the ion exchanger. In contrast, the insufficient outlet density leads to large velocity variations in the process stream. Consequently, from CFD investigations, a majority of the resin bed shows malfunctioning operations including dead space and channelling. Due to the non-uniform distribution, the process stream passes through the resin bed with a broad RTD which undermines the overall performance of the ion exchanger. From the response surface with channel width and depth scale as input parameter, we found out that 1.265 as channel aspect ratio may result in high quality of flow distribution. CFD can assist in avoiding ad-hoc design decision on dimensions and systematically explore the design space for optimum design decisions.

This study may enhance the understanding of fractal distributors and may benefit the process intensification using fractal distributors.

APPENDIX A

A snapshot of the mesh with 2.7 million elements for 1st ion exchanger. The mesh was generated with Cutcell method in ANSYS Meshing.

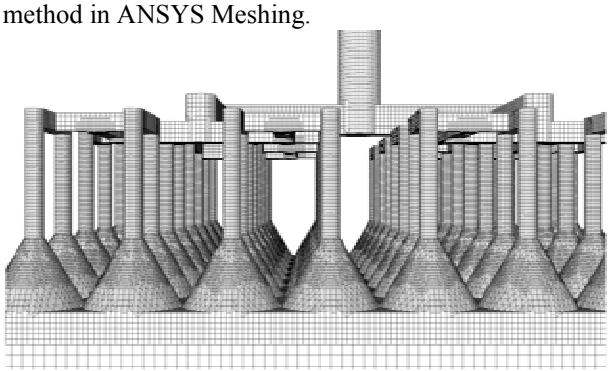

REFERENCES

INGLEZAKIS, V.J., POULOPOULOS, S.G., 2006. 3 - Heterogeneous Processes and Reactor Analysis, in: Inglezakis, V.J., Poulopoulos, S.G. (Eds.), Adsorption, Ion Exchange and Catalysis. Elsevier, Amsterdam, pp. 57-242.

KEARNEY, M.M., MUMM, M.W., PETERSEN, K.R., VERVLOET, T., (1994),"Fluid transfer system with uniform fluid distributor", US Patent. The Amalgamated Sugar Company,Ogden,Utah, U.S.

KOCHERGIN, V., KEARNEY, M., (2006), "Existing biorefinery operations that benefit from fractal-based process intensification",*Applied Biochemistry and Biotechnology*, **130**, 349-360.

LIU, H., LIANG, X., YANG, L., CHEN, J., (2010), "Challenges and innovations in green process intensification",*Science China Chemistry*, **53**, 1470-1475.

MANDELBROT, B., 1982. The fractal geometry of nature. W.H. Freeman.

T.-H. SHIH, W. W. LIOU, A. SHABBIR, Z. YANG, ZHU, J., (1995), "A New Eddy-Viscosity Model for High Reynolds Number Turbulent Flows - Model Development and Validation",*Computers Fluids*, **24**, 227-238.